*Металлофиз. новейшие технол. / Metallofiz. Noveishie Tekhnol.*
2016, т. 38, № 8, сс. 1027–1055 / DOI: 10.15407/mfint.38.08.1027
Оттиски доступны непосредственно от издателя
Фотокопирование разрешено только
в соответствии с лицензией

© 2016 ИМФ (Институт металлофизики
им. Г. В. Курдюмова НАН Украины)
Напечатано в Украине.

## ФИЗИКА ПРОЧНОСТИ И ПЛАСТИЧНОСТИ

PACS numbers: 61.72.Ff, 61.72.Hh, 62.20.Hg, 63.20.kd, 63.20.kp, 75.80.+q, 83.60.Np

# Influence of Alternating Magnetic Field on Physical and Mechanical Properties of Crystals

V. I. Karas[*,**], E. V. Karasyova[*], A. V. Mats[*], V. I. Sokolenko[*], A. M. Vlasenko[*], and V. E. Zakharov[***,****]

[*]*National Science Center 'Kharkiv Institute of Physics and Technology', N.A.S. of Ukraine, 1 Akademichna Str., 61108 Kharkiv, Ukraine*
[**]*V. N. Karazin Kharkiv National University, 4 Svobody Sq., 61022 Kharkiv, Ukraine*
[***]*P. N. Lebedev Physical Institute of the Russian Academy of Sciences, 53 Leninskiy Prosp., 119991 Moscow, Russia*
[****]*L. D. Landau Institute for Theoretical Physics of the Russian Academy of Sciences, 1-A Academician Semenov Ave., 142432 Moscow Region, Chernogolovka, Russia*

The results of the investigation of creep characteristics and activation parameters of polycrystalline nickel (of 99.996% purity) plastic flow at the temperature of 77 K are presented. The influence of nonstationary magnetic field with strength of 500 Oe (harmonic (50 Hz) and monopolar pulses of the same frequency) on the nickel creep characteristics is studied. We have deliberately conducted experimental investigations of the influence of nonstationary magnetic field of alternating and constant sign at constant temperature in order to estimate the contribution to the dislocations' mobility from the interaction of dislocations with the mobile domain boundaries as well as from the heat effects connected with the induction electric field. The proposed model of electroplastic effect (EPE) suggests the following mechanism of weakening under the action of electric field. Electric field gives energy to

Corresponding author: Vyacheslav Ignatovych Karas
E-mail: karas@kipt.kharkov.ua

Please cite this article as: V. I. Karas, E. V. Karasyova, A. V. Mats, V. I. Sokolenko, A. M. Vlasenko, and V. E. Zakharov, Influence of Alternating Magnetic Field on Physical and Mechanical Properties of Crystals, *Metallofiz. Noveishie Tekhnol.*, **38**, No. 8: 1027–1055 (2016), DOI: 10.15407/mfint.38.08.1027.

conductivity electron subsystem, making it thermodynamically nonequilibrium. Nonequilibrium electrons while interacting with acoustic phonons transfer more energy to short-wave part of the phonon spectrum. Short-wave phonons due to large stress gradient effectively detach dislocations from stoppers. Experimental results qualitatively match with the data obtained after numerical calculations.

**Key words**: magnetoplastic effect, alternating magnetic field, dislocation mobility, creep rate, ferromagnetic crystal, nonequilibrium electron and phonon subsystem.

Наведено результати досліджень характеристик плазучости та активаційних параметрів пластичної течії полікристалічного ніклю (99,996% чистоти) за постійної температури у 77 К. Досліджувався вплив нестаціонарного магнетного поля напруженістю у 500 Е (гармонічні (50 Гц) та однополярні імпульси тієї ж частоти) на параметри плазучости ніклю. Експериментальні дослідження з впливу нестаціонарного магнетного поля змінного та сталого знаку за постійної температури проводилися, щоб оцінити внесок у рухливість дислокацій від взаємодії дислокацій з рухливими межами домен, а також від теплових ефектів, пов'язаних з індукційним електричним полем. Пропонований модель електропластичного ефекту (ЕПЕ) передбачає наступний механізм знеміцнення під дією електричного поля. Електричне поле передає енергію підсистемі електронів провідности, роблячи її термодинамічно нерівноважною. Нерівноважні електрони, що взаємодіють з акустичними фононами, передають енергію переважно короткохвильовій частині фононного спектру. Короткохвильові фонони, завдяки великому ґрадієнту напруги, ефективно відкріплюють дислокації від стопорів. Результати експериментів якісно збігаються з даними числових розрахунків.

**Ключові слова**: магнетопластичний ефект, змінне магнетне поле, рухливість дислокацій, швидкість плазучости, феромагнетний кристал, нерівноважна електронна та фононна підсистеми.

Представлены результаты исследования характеристик ползучести и активационных параметров пластического течения поликристаллического никеля (99,996% чистоты) при температуре 77 К. Было изучено влияние нестационарного магнитного поля напряжённостью 500 Э (гармонические (50 Гц) и монополярные импульсы той же частоты) на параметры ползучести никеля. Экспериментальные исследования влияния нестационарного магнитного поля постоянного и переменного знака при постоянной температуре проводились с целью оценить вклад в подвижность дислокаций от взаимодействия дислокаций с подвижными доменными границами, а также от тепловых эффектов, связанных с индукционным электрическим полем. Предлагаемая модель электропластического эффекта (ЭПЭ) подразумевает следующий механизм разупрочнения под действием электрического поля. Электрическое поле передаёт энергию подсистеме электронов проводимости, делая её термодинамически неравновесной. Неравновесные электроны, взаимодействуя с акустическими фононами, передают энергию преимущественно коротковолновой части фононного

спектра. Коротковолновые фононы благодаря большому пространственному градиенту напряжения эффективно открепляют дислокации от стопоров. Экспериментальные результаты качественно совпадают с данными численных расчётов.

**Ключевые слова:** магнитопластический эффект, переменное магнитное поле, подвижность дислокаций, скорость ползучести, ферромагнитный кристалл, неравновесная электронная и фононная подсистемы.

*(Received June 13, 2016)*

## 1. INTRODUCTION

The discovery of magnetoplastic effect (MPE) [1, 2] and electroplastic effect (EPE) [3, 4] has stimulated broad study of the influence of constant and nonstationary magnetic fields on the structure and mechanical properties of ferromagnetics and antiferromagnetics [2]. MPE was being studied under the conditions of active strain and creep. The observed effects were connected with changes in dislocations dynamics during their interaction with spin subsystem and with the characteristics of the barriers.

In the sixtieth of the XX century, a phenomenon of abrupt decrease of plastic deformation resistance of metals in case of excitation of their conductivity electron subsystem by irradiation or conduction of electron current of high density, $j = 10^8$–$10^9$ A/m$^2$, was discovered. This phenomenon has been called electroplastic effect (EPE) [3]. This effect is already being applied in industry in the processes of drawing and rolling of metallic products [4–8].

## 2. STUDY OF CREEP CHARACTERISTICS AND ACTIVATION PARAMETERS OF NICKEL IN EXTERNAL NONSTATIONARY MAGNETIC FIELD

In the given paragraph, we shall present the results of the investigation of the creep characteristics and activation parameters of the polycrystalline nickel plastic flow at the temperature of 77 K. The influence of nonstationary magnetic field with strength of 500 Oe (harmonic (50 Hz) and detected (monopolar pulses of the same frequency)) upon the nickel creep characteristics was studied. Their connection with the material structural state was also analysed. We have deliberately conducted experimental researches of the influence of nonstationary magnetic field of alternating and constant sign at constant temperature in order to estimate the contribution to the dislocations mobility from the interaction of dislocations with the mobile domain boundaries and from the heat effects connected with the induction electric field.

The object of research was the polycrystalline nickel of 99.99% purity, which had been annealed at the temperature of 900°C during 2 hours. The experiments were conducted at the transient creep stage in the mode of step loading in the liquid nitrogen environment at the temperature of 77 K on the test machine with grips and pulls made of nonmagnetic material. The measurement precision was about $\cong 5 \cdot 10^{-5}$ cm. Activation parameters and internal stress level were determined by means of differential methods that are described in early works (see, for example, [2, 9–19]). The electron microscope investigations of nickel defect structure before and after magnetic field influence were carried out.

In order to study the magnetic field influence, the test specimen was placed inside a solenoid where the longitudinal magnetic field with the strength of 500 Oe was created.

In order to determine the peculiarities of the structure that had formed in the process of creep in the stress range of $\sigma \leq 0.5\ \sigma_B$, the activation parameters were investigated that allows us to make some conclusions about the type of barriers and the mechanisms that govern the nickel plastic flow during the creep process at 77 K.

Experimental researches showed that activation volume and activation energy calculated according to the thermoactivated plastic flow theory are equal to $0.72 \cdot 10^{-23}$ cm$^3$ and 0.14 eV correspondingly and decrease with the increase of stress. It means that the dislocations glide is controlled by the defects that emerge during the process of plastic flow. The whole magnitude of the activation energy necessary for the overcoming of obstacles is equal to 0.22 eV and does not depend on temperature. There are different obstacles that can control the low-temperature creep of nickel, which means that they have activation parameters close to those obtained. These are dopants, point strain defects and forest dislocations.

Though it was experimentally confirmed that the activation volume does not depend on stress, the dopants do not control the creep at 77 K. Though the concentration of point defects and dislocations increases with the increase of strain, activation volume has to decrease that is in accordance with the experiment.

Therefore, the performed experimental investigations and estimates allow us to make a conclusion that, taking into account the dislocations density in the region of dislocations bunches, forest dislocations and point defects (mostly interstitial atoms at the initial stages of plastic strain) are the barriers that control nickel low-temperature plastic flow process.

In case of the action of the magnetic field of alternating sign, the main mechanism of the nickel plastic flow at 77 K is the mechanism of thermo-activated overcoming of the obstacles, enumerated above, by dislocations. In order to change the plastic flow mechanism, we used

the action of the constant-sign magnetic field, the strength of which changed only its magnitude.

The electron microscope investigations show that the annealed nickel has strongly equilibrium structure as a result of recrystallization during annealing, which is indicated by even long traces of the grain boundaries. Dislocations density does not exceed $5 \cdot 10^8$ cm$^{-2}$. Creep at 77 K results in spatially nonuniform developing of the material flow, strong orientation dependence of the defects formation on the grain orientation relative to the direction of external stress action. For example, in some grains, a cell structure with crumbly boundaries and bunch size of 0.5–0.8 μm is observed. Average dislocations' density inside the bunches equals to $\cong 2 \cdot 10^{10}$ cm$^{-2}$ and to $\cong 9 \cdot 10^{10}$ cm$^{-2}$ in the bunch boundaries. While in the adjacent grain, one can see strong dislocation bunches of the density of $\cong 8 \cdot 10^{10}$ cm$^{-2}$.

In the same time, there are grains where only the initial stages of plastic flow with dislocation glide along the boundaries and formation in the triple junctions of bunches with dislocation density of $\cong 5 \cdot 10^{10}$ cm$^{-2}$ occurred.

The main test series with superimposing the magnetic field upon the plastic strain process was carried out according to the following schema. After applying of stress and reaching the strain rate of $\cong 5 \cdot 10^{-6}$ s$^{-1}$, the magnetic field was turned on and the creep was being detected during 180 s. After turning off the field, the creep lasted 180 s more. Then, the sample was additionally loaded again. The investigations were conducted at the transient creep stage at the stress of $\sigma \leq 0.5\sigma_B$. The creep strain obtained during 180 s after turning on the field was considered to be the magnitude of the weakening effect. Figures 1–3 demonstrate the dependence of strain on time for 2 modes of turning

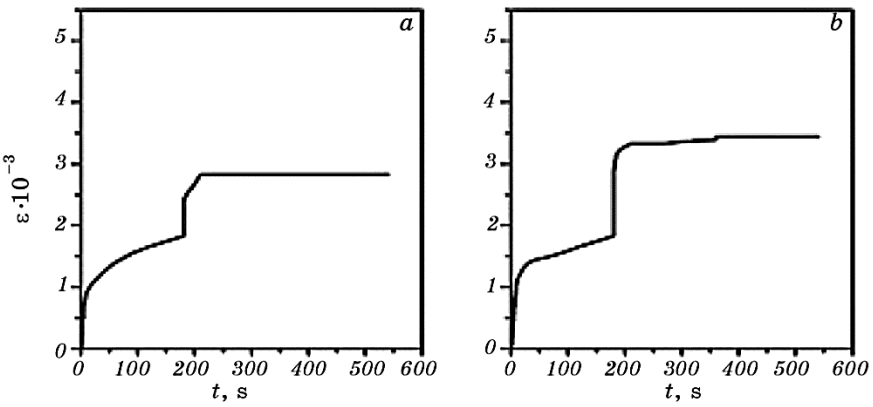


**Fig. 1.** Influence of nonstationary magnetic field of 500 Oe on the creep of nickel at 77 K and the stress of $\sigma = 0.3\sigma_B$ for different types of magnetic field pulses with $\tau = 0.005$ s: periodic monopolar pulses (*a*) and harmonic pulses (*b*).

on the nonstationary magnetic field with the increasing time of 0.005 s for periodic monopolar pulses (*a*) and of 0.005 s for harmonic pulses (*b*).

Experiments shown that turning on of the stationary magnetic field of the strength of 500 Oe during the creep of nickel specimens leads to the increase of strain, and turning off the magnetic field is also accompanied by the growth of strain. Weakening takes place with the change of magnetic field from 0 to 500 Oe and conversely. Figure 3 shows typ-

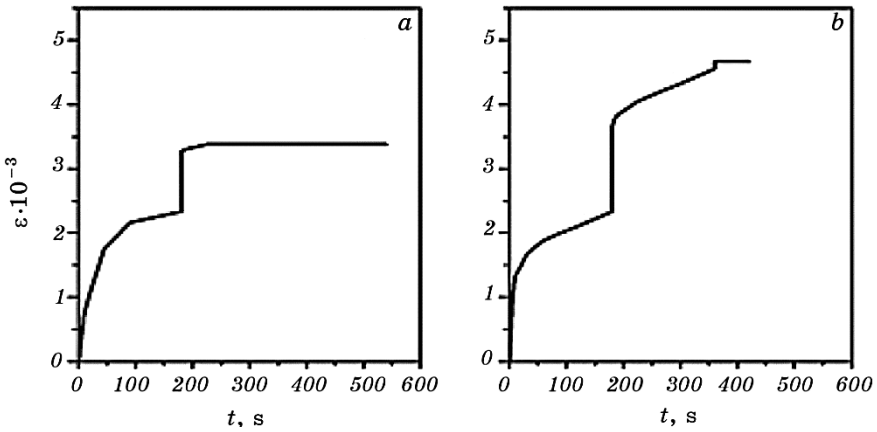


**Fig. 2.** Influence of nonstationary magnetic field 500 Oe on the creep of nickel at 77 K and the stress of $\sigma = 0.3\sigma_B$ for different types of magnetic field pulses with $\tau = 0.005$ s: periodic monopolar pulses (*a*) and harmonic pulses (*b*).

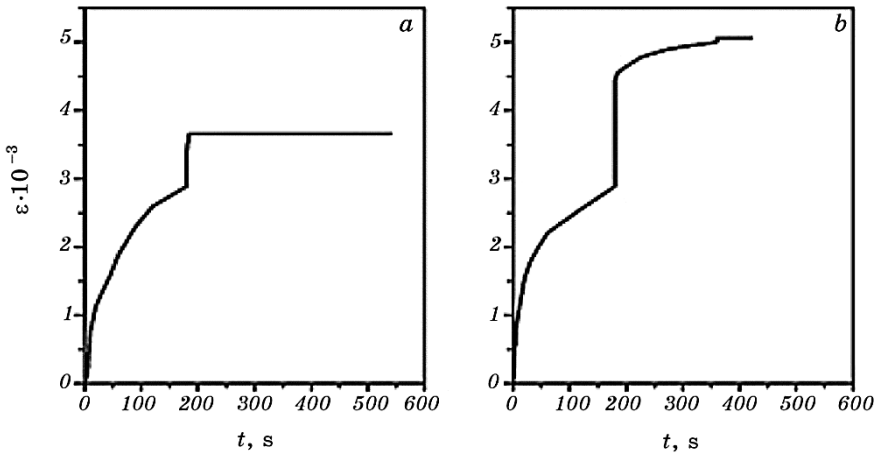


**Fig. 3.** Influence of nonstationary magnetic field of 500 Oe on the creep of nickel at 77 K and the stress of $\sigma = 0.5\sigma_B$ for different types of magnetic field pulses with $\tau = 0.005$ s: periodic monopolar pulses (*a*) and harmonic pulses (*b*).

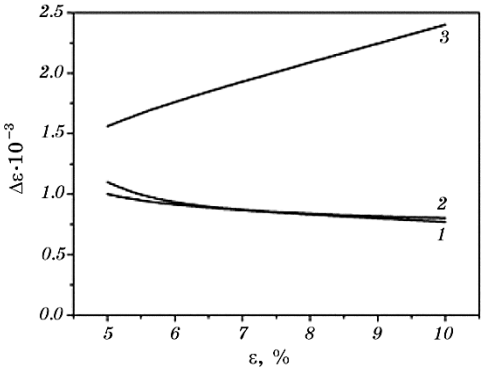


**Fig. 4.** Dependence of the polycrystalline nickel weakening magnitude at 77 K in stationary magnetic field with the growth time of 1 s (*1*), periodic monopolar pulses (*2*) and harmonic magnetic field (*3*) of the strength of 500 Oe upon strain degree.

ical nickel creep curves change as a result of turning on and off the nonstationary magnetic field of the strength of 500 Oe with different growth time under the strength of $\sigma = 0.5\sigma_B$. One can see that after turning on and off the magnetic field with different growth time the form of the creep curves changes essentially: the lesser the growth time the greater the strain rate jump for each investigated value of strength. Let us mention that the case (*a*) corresponds to short monopolar pulses.

Figure 4 illustrates the manifestation of the nickel weakening effect at different modes of the magnetic field action.

Figure 4 also shows that weakening under the action of monopolar

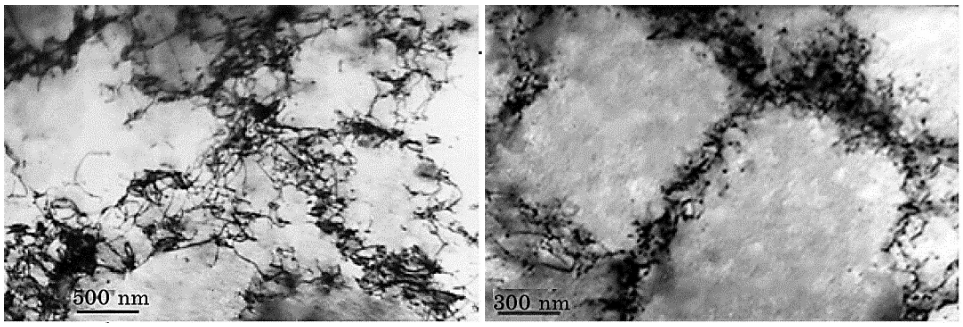


**Fig. 5.** Dislocation structure of nickel after the 9% strain under the conditions of stage creep at $T = 77$ K and superposition of nonstationary magnetic field of 500 Oe with different field growth time $\tau$: $\tau = 60$ s (*a*) (single pulse), $\tau = 0.005$ s (periodic monopolar pulses) (*b*).

pluses and stationary field with the growth time of 1 s practically coincides in a wide range of creep strain stages. In case of harmonic pulses, the weakening grows essentially with the increase of strain.

Electron microscope investigation showed that nonstationary magnetic field influences the material structure the stronger the lesser the field growth time is (see Fig. 5). The body of bunches is cleaned from dislocations and they concentrate only on the boundaries (Fig. 5, *b*). Dislocation density on the boundaries greatly exceeds $10^{11}$ cm$^{-2}$ and cannot be distinguished by the methods of electron microscopy and near the grain boundaries strong dislocation bunches are formed (see Fig. 5, *b*).

## 3. THEORETICAL INVESTIGATION OF WEAKENING OF NICKEL AT CREEP IN NONSTATIONARY MAGNETIC FIELD

### 3.1. About the Influence of Phonons on Dislocations

Plastic deformation of crystals under the action of external loads in most cases is accomplished by dislocation glide. The main equation describing the kinetics of the process of the plastic deformation—the Orovan modified equation (see, for example, [20]):

$$\dot{\varepsilon}_d = bl\rho_d \nu_d(\sigma^*), \quad \sigma^* = \sigma - \sigma_i, \tag{1}$$

where $\dot{\varepsilon}_d$ is the strain rate, $|\mathbf{b}|$—the Burger's vector, $l$—the mean distance between stoppers, $\rho_d$—the mobile dislocations density, $\nu_d(\sigma^*)$—the frequency of the stoppers overcoming by dislocations, $\sigma^*$—the effective shear stress, $\sigma_i$—the internal shearing stress in the glide plane.

For the case of thermodynamic equilibrium, the expression for $\nu_d(\sigma^*, T)$ has the form of

$$\nu_d(\sigma^*, T) = \nu_d^0 \exp\left(-\frac{H(\sigma^*)}{k_B T}\right), \tag{2}$$

where $k_B$ is the Boltzmann constant and $T$ is the temperature.

The explicit form of the $H(\sigma^*)$ function depends on the potential barrier model. For the consideration of a more general case, *i.e.* when electron and phonon subsystems can be, generally speaking, in the state of nonequilibrium, the Landau–Hoffman model will be used [21]. The potential pit has parabolic form

$$U(x) = \begin{cases} \zeta x^2, & |x| \le x_{\text{cr}}, \\ 0, & |x| > x_{\text{cr}}, \end{cases} \tag{3}$$
$$\zeta x_{\text{cr}} = U_0.$$

The displacement of the dislocation segment of length $L$ under the stress σ will be described in the approximation of the elastic string vibrations (Granato–Lücke model [22]):

$$M\frac{\partial^2 u}{\partial y^2} + B\frac{\partial u}{\partial t} - C\frac{\partial^2 u}{\partial y^2} = b\sigma + f(t). \tag{4}$$

Here, $u(y, t)$ is the displacement of the dislocation line at the point $y$ in the direction $x$, $M = \frac{\rho b^2}{2}$ is the effective mass of the length unit, ρ is the material density, $B$ is the coefficient of the dynamic friction force per unit of length, $C = \frac{Gb^2}{2}$ —the linear tension of the string, $G$ is the shear modulus, $f(t)$ is the force of the random pushes that are exerted by crystal upon the unit of dislocation length.

Boundary conditions are:

$$u'(0,t) = ku(0,t), \quad -u'(L,t) = ku(L,t), \quad k = \frac{2\zeta}{C}. \tag{5}$$

The equation (4) is linear, so its solution can be written as a sum

$$u(y,t) = u_{\text{st}}(y) + u_{\text{osc}}(y,t),$$

where $u_{\text{st}}(y)$ is the static deflection, caused by external stress σ, and $u_{\text{osc}}(y, t)$ are the oscillations under the action of a random force

$$u_{\text{st}}(y) = \frac{by(L-y)}{2C} + \frac{bL\sigma}{2Ck}, \quad u_{\text{osc}}(y,t) = \sum_{n=1}^{N} Q_n(t)\left(\sin(q_n y) + \frac{q_n}{k}\cos(q_n y)\right),$$

$$\operatorname{ctg}(q_n y) = \frac{q_n^2 - k^2}{2q_n k}. \tag{6}$$

The quantity of $Q_n(t)$ satisfies the following equation

$$M\ddot{Q}_n(t) + B\dot{Q}_n(t) + M\omega_n^2 Q_n(t) = f_n(t), \quad \omega_n^2 = q_n^2\frac{C}{M}. \tag{7}$$

Let us consider a ‘fixing point’ at $y = 0$. Let the segment lengths on both sides of it be equal to $L$. Then, the total deflection at the ‘fixing point’ is equal to

$$u(0,t) = 2u_{\text{st}}(y) + 2u_{\text{osc}}(y,t) = \tilde{u}_{\text{st}}(y) + \tilde{u}_{\text{osc}}(y,t). \tag{8}$$

The case of a random force was considered in the work [22]. We shall now provide some of the calculations for the reference purpose. If, at

some time moment, a random event occurs such that $\delta\tilde{u}(0,t) \geq \delta\tilde{u}_{\text{cr}}$, then, the condition of obstacle overcoming in the direction on the loading action will be satisfied. Let $f_n(t)$ be a stationary Gauss process. Since the equation (7) is linear, $Q_n(t)$ and correspondingly $\delta\tilde{u}(0,t)$ is also stationary Gauss process for which the mean number of exceeding a particular quantity $\delta\tilde{u}_{\text{cr}}$ per unit of time is equal to

$$\nu = \frac{1}{2\pi}\sqrt{-\frac{\Psi''(0)}{\Psi(0)}}\exp\left\{-\frac{\delta\tilde{u}_{\text{cr}}^2}{2\Psi(0)}\right\}, \tag{9}$$

$$\Psi(\tau) = 2\sum_{n=1}^{\tilde{n}}\frac{q_n^2}{k^2}\overline{Q_n(t)Q_n(t+\tau)} \equiv 2\sum_{n=1}^{\tilde{n}}\frac{q_n^2}{k^2}\psi(\tau), \tag{10}$$

$$\delta\tilde{u}_{\text{cr}} = x_{\text{cr}} - \frac{bL\sigma}{Ck} = x_{\text{cr}}\left(1 - \frac{\sigma}{\sigma_{\text{cr}}}\right), \quad \sigma_{\text{cr}} \equiv \frac{Ckx_{\text{cr}}}{bL}, \tag{11}$$

where $\Psi(\tau)$ is the random process $\delta\tilde{u}(0,t)$ correlation function expressed by means of random process $Q_n(t)$ correlation function $\psi(\tau)$; $\Psi''(0)$ is the second derivative with respect to $\tau$ at $\tau = 0$. For the Fourier components $(Q_n)_\omega$ of $Q_n(t)$, we can write

$$\psi(\tau) = \int_{-\infty}^{\infty}(Q_n)_\omega^2 e^{-i\omega\tau}d\omega, \tag{12}$$

where the definition of the quantity $(Q_n)_\omega^2$ is given by the relation

$$\overline{(Q_n)_\omega(Q_n)_{\omega'}} = (Q_n)_\omega^2\delta(\omega - \omega'). \tag{13}$$

Each harmonic can be formally considered as an independent vibrator with friction $\chi$ and frequency $\omega_n$:

$$m\ddot{Q} + \chi\dot{Q} + m\omega_n^2 Q = F, \tag{14}$$

where $m$ is the proportionality coefficient between the generalized momentum and velocity $\dot{Q}$, $\chi$ is the friction coefficient, $F$ is the random force [22]

$$m = M\frac{L\xi_n}{2}, \quad \chi = B\frac{L\xi_n}{2}, \quad F = f_n\frac{L\xi_n}{2}, \quad \xi_n = 1 - \frac{2}{kL} + \frac{q_n^2}{k^2}. \tag{15}$$

Therefore, for the Fourier component, we obtain the following formula:

$$(Q_n)_\omega^2 = \frac{(F_\omega)^2}{m^2(\omega_n^2 - \omega^2)^2 + \chi^2\omega^2}. \tag{16}$$

Random force spectral density can be found from the expression [23]

$$(F_\omega)^2 = \frac{\chi}{\pi}\hbar\omega\left(\frac{1}{2} + N(\omega)\right). \tag{17}$$

Hence, to estimate the force exerted by phonons upon dislocations, one must first find the phonon distribution function $N(\omega)$ [24–29].

### 3.2. Nonequilibrium Kinetics of Electron–Phonon Subsystem

Though we investigate the behaviour of a sample in harmonic and nonstationary magnetic field, it is important to estimate the influence of eddy electric field, induced by nonstationary magnetic field, upon the change of the mechanical properties of the sample [30]. Using the Maxwell equations, we can estimate the characteristic magnitude of the electric field

$$\begin{aligned} &\mathrm{rot}\mathbf{E} = -\frac{1}{c}\frac{\partial}{\partial t}(\mu\mathbf{H}), \quad E_0 = \frac{4\pi H_0}{\tau c} l_x(\mu + H_z H_z), \\ &H_z = H_0 \left|\sin(\pi t / 2\tau)\right|, \quad \mu = \mu(H_z(t), t), \end{aligned} \tag{18}$$

where $\tau$ is the magnetic field growth time, $l_x$ is the sample width, $l_x = 3$ mm. The width of the sample $l_x$ is much greater than its thickness $l_y = 0.3$ mm.

Besides, let us estimate the maximal contribution from the longitudinal magnetostriction that is usually taken into account [19]. Magnetostrictive strain can be neglected because: i) it has opposite sign (so it cannot help us elongate our sample); ii) its magnitude does not exceed $10^{-4}$.

For simplicity, while solving the set of kinetic equations for electrons and acoustic phonons, we consider spatially uniform electric field as well as distribution functions of electrons and phonons. Electron distribution function becomes isotropic as a result of electron-dopant collisions [24, 25]. In this case, we can neglect the umklapp processes. In case of relatively small electric fields, the contribution from electron–phonon collisions greatly exceeds the contribution from electron–electron interaction, and therefore hereinafter, at small time intervals, the electron–electron collisions will not be taken into account [23–25].

For the phonon distribution function, we also take into account the finite lifetime of phonons (second term in (19)) in our system

$$\tau\frac{\partial N(\mathbf{q})}{\partial t} = I_{\mathrm{pe}} = -\frac{N_0(\mathbf{q}) - N(\mathbf{q})}{\tau_b}, \tag{19}$$

where $I_{\text{pe}}$ is the phonon–electron collision integral [24–27], $N_0(\mathbf{q}) = [\exp(\hbar\Omega / k_B T) - 1]^{-1}$ is the thermodynamically equilibrium phonon distribution function—Bose–Einstein function at $T_0$, $T_0 = 77$ K is the temperature of liquid nitrogen, $\hbar\Omega(q) = sq$, $\mathbf{q}$ is the phonon momentum, $s$ is the transverse sound velocity, $\tau_b = (s/s_{N2})^2 l_y / 2s$, $sN_2 = 8.67 \cdot 10^4$ cm/s is the sound velocity in liquid nitrogen.

In the considered case, the frequency of electron-phonon collisions is much less than the frequency of the collisions of electrons with defects. Collisions with defects and dopants occur very often, at time intervals small compared to the characteristic phonon–electron interaction time. That is why the anisotropic additive can be considered stationary and spatially uniform. As a result, we obtain the final set of two equations for isotropic distribution functions of electrons and acoustic phonons [24, 25, 27–29], which is to be solved without Tailor expansion of electron distribution function

$$\frac{\partial f}{\partial \tilde{t}} - 4\Delta\tilde{\varepsilon}\frac{1}{\tilde{\varepsilon}^{\frac{1}{2}}}\frac{\partial}{\partial\tilde{\varepsilon}}\left[\tilde{\varepsilon}^{\frac{3}{2}}\frac{\partial f}{\partial\tilde{\varepsilon}}\right] =$$

$$= \frac{1}{8}\alpha^{-\frac{5}{2}}\frac{1}{\sqrt{\tilde{\varepsilon}}}\int_0^{\varepsilon_-} d\tilde{\varepsilon}_{ph}\tilde{\varepsilon}_{ph}^2\left[f(\tilde{\varepsilon}-\tilde{\varepsilon}_{ph})N(\tilde{\varepsilon}_{ph}) + f(\tilde{\varepsilon})\left(f(\tilde{\varepsilon}-\tilde{\varepsilon}_{ph}) - 1 - N(\tilde{\varepsilon}_{ph})\right)\right] +$$

$$+\frac{1}{8}\alpha^{-\frac{5}{2}}\frac{1}{\sqrt{\tilde{\varepsilon}}}\int_0^{\varepsilon_+} d\tilde{\varepsilon}_{ph}\tilde{\varepsilon}_{ph}^2\left[f(\tilde{\varepsilon}+\tilde{\varepsilon}_{ph})[N(\tilde{\varepsilon}_{ph})+1] - f(\tilde{\varepsilon})(f(\tilde{\varepsilon}+\tilde{\varepsilon}_{ph}) + N(\tilde{\varepsilon}_{ph}))\right], \quad (20)$$

$$\frac{\partial N(q)}{\partial\tilde{t}} = \frac{1}{2\alpha}\int_{\varepsilon_0}^{\infty} d\tilde{\varepsilon}\left[(f(\tilde{\varepsilon}+\tilde{\varepsilon}_{ph}) - f(\tilde{\varepsilon}))N(\tilde{\varepsilon}_{ph}) + f(\tilde{\varepsilon}+\tilde{\varepsilon}_{ph})(1-f(\tilde{\varepsilon}))\right] -$$

$$-\frac{N_0(q)-N(q)}{\tau_b}. \quad (21)$$

Here, the following designations are used:

$$\alpha = \frac{ms^2}{2k_B T_e},\ \Delta\tilde{\varepsilon} = \frac{e^2E^2\tau_{ep0}}{6m\nu_{ed}k_B T_e},\ \tilde{\varepsilon} = \frac{\varepsilon}{k_B T_e},\ \tilde{p} = \frac{p}{\sqrt{2mk_B T_e}},\ \tilde{\varepsilon}_{ph} = \frac{\varepsilon_{ph}}{k_B T_e},$$

$$\tilde{t} = \frac{t}{\tau_{ep0}},\ \tau_{ep0} = \frac{(2\pi\hbar)^3\hbar\rho}{\pi m^3 s\varepsilon_{1A}^2} = 3.446\cdot 10^{-7}\text{s}.$$

Integration limits, which are obtained with respect to energy conservation law, are correspondingly equal to

$$\varepsilon_- = \min\left[4(\sqrt{\tilde{\varepsilon}\alpha} - \alpha),\ \tilde{\varepsilon}_{ph_D}\right],\ \varepsilon_+ = \min\left[4(\sqrt{\tilde{\varepsilon}\alpha} + \alpha),\ \tilde{\varepsilon}_{ph_D}\right],$$

$$\varepsilon_0 = \frac{\tilde{\varepsilon}_{ph}^{\,2}}{16\alpha} - \frac{\tilde{\varepsilon}_{ph}}{2} + \alpha. \tag{22}$$

Distribution functions of electrons, $f(\varepsilon)$, and phonons, $N(q)$, are dimensionless quantities, which satisfy the following normalizing conditions:

$$\frac{1}{2\pi^2}\left(\frac{2m}{\hbar^2}\right)^{\frac{3}{2}} \int_0^{\infty} \varepsilon^{\frac{1}{2}} f(\varepsilon) d\varepsilon = n, \tag{23}$$

where $n$ is the electron concentration in the valence band (for metals also conduction band, which is only partially filled);

$$\frac{1}{2\pi^2}\left(\frac{1}{\hbar^3}\right) \int_0^{q_D} q^2 N(q) dq < \infty, \tag{24}$$

where $q_D$ is the momentum of Debye phonon, which is defined by the expression

$$q_D = \frac{\pi\hbar}{a}\sqrt{2}. \tag{25}$$

All the quantities are taken for nickel: $s = 2.96 \cdot 10^5$ cm/s is the transversal sound velocity, $n = 2.5 \cdot 10^{22}$ cm$^{-3}$ is the electron concentration in the conduction band, $a = 3.5 \cdot 10^{-8}$ cm is the lattice parameter, $\rho_s^{-1} = 0.333 \cdot 10^6$ S/cm is the specific residual resistance.

Thermodynamically equilibrium electron energy distribution function is the Fermi–Dirac function:

$$f_0(\varepsilon) = \left[\exp\left(\frac{\varepsilon - \varepsilon_F}{k_B T_e}\right) + 1\right]^{-1}, \tag{26}$$

where $\varepsilon_F = 5 \cdot 10^{-19}$ J is the Fermi energy for nickel, $T_e$ is the initial electron temperature 77 K.

## 4. COMPARISON OF DIFFERENT THEORETICAL MODELS WITH EXPERIMENTAL DATA

Electroplastic effect, *i.e.* the phenomenon of weakening of metals during plastic strain while conducting high-density electric pulses, has been known more than 50 years already. This phenomenon is widely used in manufacturing of different metallic products. Though the influence of different parameters upon the magnitude of this effect is experimentally studied, there exists no sole quantitative theory yet.

In this section, we compare our approach with those most widely

used for explanation of the electroplastic effect. In the first subsection, we review the works of Hans Conrad and co-authors [31]. They approach to the explanation of EPE from the point of view of the electron wind theory, *i.e.* the direct action of drift conductivity electrons upon the dislocation motion. Experiments are conducted, as a rule, at constant strain rate. Based on the measured mechanical loading drop that accompanied the conduction of current pulse, the authors determine the electron drag coefficient and compare it to that predicted theoretically.

The second subsection deals with the Michel Molotskii's theory, which is presented in his articles [32–34]. In his earlier works, Molotskii considered the influence of magnetic field on the interaction of dislocations with paramagnetic dopants-stoppers. From the point of view of this model, electroplastic effect emerges as a result of the influence of the self-magnetic field generated by the current. The author has made some mathematical inaccuracies that will also be considered and corrected as far as possible.

Third subsection is about the approach of Bilyk *et al.* [35]. Their conclusions contradict the prior works, in particular those reviewed in this report. Therefore, the authors think that it is thermal expansion due to Joule heating, which plays the key role. Direct influence of current upon dislocations, if it exists, is considered by the authors to be secondary effect.

### 4.1. Influence of the Electric Current Density upon the Plasticization of Metals

The influence of high-density ($10^5$ A/cm$^2$) current pulses upon the plastic flow stress of polycrystalline metals at axial strain was researched in the article [31]. Pulse duration was 60 μs. Temperature 300 K. The observed increase in dislocation mobility was explained by the action of drift electrons.

**Experiment.** At first, the samples were deformed at constant strain rate of $1.7 \cdot 10^{-4}$ s$^{-1}$ until the degree of strain that is slightly lower than it was desired. Then, the elasticity modulus of the test machine was measured. After that, the plastic strain of the sample went on until the necessary strain degree while two current pulses within the interval of 10 s were passed through the sample. Loading drops $\Delta\sigma_f$ were observed. Then, the sample was unloaded to the level of long-range internal stress, and for current, pulses within the interval of 60 s were passed through it. It was accompanied by the stress drops $\Delta\sigma_e$. Then, the routine was repeated for the higher degree of strain. $\Delta\sigma_e$ is the contribution to the loading drop from the elastic strain caused by such 'side' effects of current as pinch effect, skin effect, magnetostriction and thermal expansion due to Joule heating. So, the difference $\Delta\sigma_p = \Delta\sigma_f -$

$-\Delta\sigma_e$ is the contribution from the plastic strain.

The dependence of loading drop $\Delta\sigma_p$ on strain degree was determined. For body centred cubic (b.c.c.) metals, the dependence is descendant. For face centred cubic (f.c.c.) metals, the dependence was absent. For b.c.c. nickel and titan, the dependence was nonmonotonic. The flow stress after passing of the current pulse returned to its previous value that testifies that no significant change in dislocation structure of the sample occurred as a result of current pulse passing.

The behaviour of metals and alloys under the influence of high-density current pulses and stationary electric field was studied in the work [31]. In the theoretical part, special attention was payed to the consideration of dislocation motion under the influence of electron wind.

Pulse current with the current density of $10^3$–$10^6$ A/cm$^2$ and pulse duration of 100 μs was applied. The increase of strain rate at low homological temperatures under the action of pulse current was observed. The fatigue life increased. In addition, the recrystallization rate increased.

It was ascertained that conducting of current pulses of density of the order of $10^5$ A/cm$^2$ and duration under 100 μs increases plastic strain rate.

**The Influence of Pulse Current.** Direct dependence of the effect magnitude on the prior strain rate was revealed. The investigations were conducted with niobium at the temperature of 300 K in the strain rate range from $1.7\cdot10^{-5}$ to $8.4\cdot10^{-4}$ s$^{-1}$.

Conducting of current pulses of the density of $1.3\cdot10^4$ A/cm$^2$ during rotational bending of Ni and Cu samples caused the 1.2–3 times increase of their durability, which was manifested by the increase of the number of loading cycles needed for microcrack formation, and also by the decrease of the crack growth rate. Influence of the pulse current also revealed itself by increase of the slip band density.

Conduction of $10^5$ A/cm$^2$ density, 100 μs duration and 2 s period current pulses through copper during annealing increased the recovery and recrystallization rate and decreased the grain growth rate. Recrystallization of more fine grains took place. The magnitude of recrystallization rate increase decreased with the increase of the time of prior cold working. Pulse current accelerated the recrystallization kinetics at the cost of pre-exponential factor without essentially influencing the activation energy. Maximal temperature rise due to Joule heating did not exceed 2 K. Similar effects were observed also at annealing of high purity (99.996%) and commercial purity (99.8%) Al, and intermetallic compound $Ni_3Al$ containing boron. The pulse current influence upon recrystallization is prescribed to its influence upon the formation and merging of subgrains.

Conduction of current pulses (density $10^5$ A/cm$^2$, duration 60–95 μs

and frequency 4.2–8.7 Hz) through the samples of two amorphous iron-based alloys (Fe75Si10B15 and Fe79Si7B14) caused the precipitation of α-iron at temperatures, which were more than 150 K less than those at which iron crystallization without electric current is observed. Possible reason—enhanced diffusion rate (electromigration).

Sintering of aluminium powder under the conditions of conduction of $2.7 \cdot 10^5$ A/cm$^2$, 10 μs duration and 1 pulse per 30 s frequency electric current pulses caused 30% decrease of porosity.

Direct current influence was discussed in the work [31].

Adding of stationary kV/cm electric field caused slowing down recrystallization and recovery processes in Al and Cu that underwent cold working. Grain growth and void formation during superplastic strain of Al7475 alloy was also decelerated. Quench ageing, bainite formation and steel tempering processes were also slowed.

The contrary was observed in case of $Ni_3Al$ alloy — acceleration of recrystallization and recovery. Ascending dependence of electroplastic strain magnitude on strain rate was observed.

Direct $6.5 \cdot 10^2$ A/cm$^2$ density current has slightly increased the tempering if 0.9C instrumental steel. The effects of alternating 60 Hz and pulse current were yet less. Pulses of current ($j = 2.3 \cdot 10^5$ A/cm$^2$, 10 μs duration, 1 pulse per 30 s) during the sintering of cold pressed aluminium powder samples caused the 30% porosity decrease.

Applying of stationary electric field $E$ = 2 kV/cm to the sample of Al7475 alloy that was undergoing superplastic strain at the temperature of 520°C caused such effects: a) flow stress drop; b) deformation strengthening rate decrease; c) slight increase of deformation strengthening exponent; d) fourfold decrease of void volume fraction in the 1.2 mm thick sample. The mechanism of those effects was not entirely clear, because the magnitude of electric field in the bulk of sample has to be zero.

Adding of 2.4–8 kV/cm electric field during isochronal annealing of Cu and Al resulted in the increase of recovery and recrystallization temperatures, despite of the fact that the field damped those phenomena (contrariwise to the pulse current effect). In a sufficient stress-field strength range, the effect has not been revealed. In addition, we have no dependence on dielectric constant of the medium containing sample. The above-mentioned effects took place not only at the surface but also in the bulk of the sample.

10 kV/cm electric field slowed quench aging of 99.9% iron.

1–2 kV/cm electric field applied at the quench strengthening and tempering of steel 4 340, as well as instrumental steel 02(0.9C), caused the following effects: a) growth of austenisation rate; b) quenching enhancement; c) slight decrease of tempering rate. In case of tempering in a mineral oil, the electric field had such influence on microstructure: a) slight refinement of austenite grains; b) decrease of upper

bainite fraction; c) decrease of microtwins' density in martensite. Above-mentioned effects were observed in the bulk of 2–3 mm thick sample as well as at its surface.

Skin effect, pinch effect and magnetostriction were taken into account. In all cases, the skin depth has exceeded the samples radii, which were equal to 0.17–0.25 mm several times. So, the current was distributed practically uniformly over the sample cross-section.

The contribution of pinch effect to the load drop was 0.25–0.77 MPa that is small compared to total load drop.

The contribution of magnetostriction was also small.

The heating of the sample was measured by means of thermocouple. Authors [31] consider Joule heating to be the most important of the current influence side effects. It is Joule heating that makes crucial contribution to the magnitude of reversible strain. Temperature raise under the condition of adiabatic heating ranged from 5 (copper) to 160 (titanium) K for the 5500 A/mm$^2$ density of current. The magnitude of loading drop due to thermal expansion turned out to be only slightly less than the measured $\Delta\sigma_e$.

Alongside with side effects electric current also exerted direct influence on material plastic flow. The magnitude of the additional force, caused by this effect, is compared to the magnitude of 'electron wind' force, calculated according to three different models. A match by the order of magnitude with Roshchupkin's model was obtained. Other two models predict the magnitude two orders less than observed.

Authors think that the effect consists of the 'electron wind' force, which is proportional to the current density, and of the effect of unclear nature, the contribution of which is proportional to the current density squared. Strain rate change is described by the following formula

$$\frac{\dot{\varepsilon}_j}{\dot{\varepsilon}_a} = \alpha j^2 \exp(\beta j), \tag{27}$$

where $\dot{\varepsilon}_a$ and $\dot{\varepsilon}_j$ are strain rates before and during conduction of current pulses of density $j$ correspondingly, $\alpha$ and $\beta$ are the material parameters.

Electron wind force per unit of dislocation length for Al and Cu has the following form:

$$F_{ew} = K_{ew} j, \text{ where } K_{ew} = 5 \cdot 10^{-8} \text{ (dyne/cm)/(A/cm}^2\text{)}. \tag{28}$$

Electron drag coefficient can contain phonon component, which emerges due to the interaction of drift electrons with the phonons. Because of electron–phonon collisions, a nonstationary phonon flux in the direction of current can emerge. Force excreted by phonon flux upon dislocation, being added to the electron drag force, can assist dislocations in overcoming obstacles.

Other possibility is connected with the influence of electric current upon the stacking fault. Its decrease would cause the increase of mobile dislocations velocity.

Except electron wind, drift electrons can also influence thermoactivation parameters. This effect depends on the current density squared.

### 4.2. Influence of the Electric Current Density on the Plasticization of Nonferromagnetic Materials

Michel Molotskii in his works [32–34] proposes the following model of the influence of magnetic field upon the plastic properties of the material. Electroplastic effect, according to Molotskii, is a particular manifestation of magnetoplastic effect, when the magnetic field is created by the electric current. That is why Molotskii considers only the influence of the magnetic field.

According to his model, magnetic field changes the mutual orientation of spins of the dislocation core and paramagnetic dopant. Antiparallel spin orientation is characterized by the strongest bond. In the states with different spin orientations, the binding energy is essentially less that eases the depinning of dislocations from the dopants.

Without the magnetic field, each of the four possible mutual spin orientations is realized with the equal probability. Imposing of the magnetic field causes the increase of the number of weakly coupled radical pairs that is equivalent to the decrease of the dopant concentration. Molotskii finds the dependence of the population of certain spin sates on the magnitude of the magnetic field.

$$\rho_{ss}(H) = \frac{1}{4}\frac{\left(1+\frac{T_1}{\tau}\right)\left(1+\frac{T_2}{\tau}\right)+\frac{1}{2}\left(\frac{H}{H_m}\right)^2}{\left(1+\frac{T_1}{\tau}\right)\left(1+\frac{T_2}{\tau}\right)+\left(1+\frac{\tau}{2T_1}\right)\left(\frac{H}{H_m}\right)^2}, \quad H_m = \frac{\hbar}{\Delta g \mu_B \sqrt{T_1 T_2}}, \tag{29}$$

where $T_1$ and $T_2$ are the characteristic times of the longitudinal and transversal spin relaxation, $\tau$ is the average time for the radical pair to pass the resonance region. Introducing the following designations

$$H_0 = 2H_m\sqrt{\frac{T_1}{\tau}\left(1+\frac{T_2}{\tau}\right)}, \quad \alpha = 2\frac{2T_1+\tau}{T_1+\tau},$$

we can rewrite this formula in a more compact form

$$\frac{\rho_{ss}(H)}{\rho_{ss}(0)} = 1 - \frac{2H^2}{H_0^2 + \alpha H^2}. \tag{30}$$

The next step in the given model is to find the connection between the field magnitude and the dislocation mean free path. In the work [34], the inverse relationship between dislocation mean free path and dopant concentration is suggested.

In the article [34], the dislocation mean free path is suggested to be inversely proportional to the square root of the dopant concentration

$$l(H) = l(0)\sqrt{\frac{\rho_{ss}(0)}{\rho_{ss}(H)}}. \tag{31}$$

With substituting (30), we obtain

$$l(H) = l(0)\left(1 - \frac{2H^2}{H_0^2 + \alpha H^2}\right)^{-1/2}. \tag{32}$$

From this moment, Molotskii considers the limit case. With respect to the limit of small field, he obtains the expression for the change of dislocation mean free path

$$\frac{l(H)}{l(0)} = 1 + \frac{H^2}{H_0^2}. \tag{33}$$

Here, the attention should be payed to the disappearing from the formula (32) of the term with $\alpha$ ($2 < \alpha < 4$).

In order to determine the dependence of the drop of the deforming stress at the plastic strain at constant rate on the magnitude of the applied magnetic field, the author uses the following empiric dependence:

$$\sigma(H)l(H) = \sigma(0)l(0). \tag{34}$$

As a result of substitution of the relation found above, Molotskii obtains the following dependence of the stress drop magnitude on the magnetic field strength

$$\frac{\Delta\sigma(H)}{\sigma(0)} = \frac{H^2}{H^2 + H_0^2}. \tag{35}$$

Taking into account the previous remark withholding the $H^2$-term in the denominator exceeds the precision of chosen approximation, so this term should have been discarded as

$$\frac{\Delta\sigma(H)}{\sigma(0)} = \frac{H^2}{H_0^2}. \tag{35a}$$

Then, Molotskii uses the obtained relation for explanation of the electroplastic effect, by substituting the value of magnetic field, cre-

ated by the electric current of given density.

$$H = \frac{1}{2} jr, \quad H_0 = \frac{1}{2} j_0 r. \tag{36}$$

He obtains the following relation

$$\frac{\Delta\sigma(j)}{\sigma(0)} = \frac{j^2}{j^2 + j_0^2}. \tag{37}$$

The term in the denominator, considering the remarks regarding (35), should also be discarded. The following should have been obtained

$$\frac{\Delta\sigma(j)}{\sigma(0)} = \frac{j^2}{j_0^2}. \tag{37a}$$

At the transition from (35) to (37), we have taken into account the fact that in case of current density that is uniformly distributed over the cross-section of the conductor, the value $H$ of the magnetic field strength grows with the distance from the axis of the sample. But, the parameter $H_0$ is the property of the material and depends neither of the size of the sample, nor on the coordinates in the bulk of this sample. If letter '$r$' in (36) designates the wire radius, then, (37) with respect to substitution (36) has the meaning of relative stress drop in the circular layer near the conductor's surface. If $r$ is the polar radius that varies from 0 to the radius of the sample, then, $j_0$ is not a constant and does depend on $r$.

Considering this, expression (37) should have the following form

$$\frac{\Delta\sigma(j,r)}{\sigma(0)} = \frac{\frac{1}{4} j^2 r^2}{\frac{1}{4} j^2 r^2 + H_0^2}, \tag{38}$$

Or, introducing the characteristic current density $j_0$,

$$\frac{\Delta\sigma(j,r)}{\sigma(0)} = \frac{\left(r/R_0\right)^2}{\left(r/R_0\right)^2 + \left(j_0/j\right)^2}. \tag{39}$$

Here, a substitution was made

$$H(r) = \frac{jr}{2}, \quad H_0 = \frac{j_0 R_0}{2}. \tag{40}$$

It is worth to underline the difference between $r$ and $R_0$ in this substitution; $r$ is the polar radius that changes from 0 to $R_0$, where $R_0$ is the radius of the wire. As well as $H_0$, $j_0$ does not depend on the polar ra-

dius. But, on the contrary to $H_0$, $j_0$ depends on the size of the sample. Therefore, although we have transited to the notation in terms of characteristic current density, we should remember that it is the characteristic magnetic field $H_0$ that has crucial physical meaning.

Results predicted by this model are then compared to the experimental data on electroplastics. Experiments give square dependence of stress drop on current density at small current densities. Molotskii also obtains square dependence, expanding (37) with respect to small $j$:

$$\Delta\sigma(j) = \sigma^* \frac{j^2}{j_0^2}. \tag{41}$$

After substituting $j_0$ from (36), the dependence of the radius of round wire being deformed has been obtained

$$\Delta\sigma(j) = \frac{1}{4}\sigma^* \frac{j^2 R_0^2}{H_0^2}. \tag{42}$$

Here, $R_0$ is the radius of the wire.

Experiments show saturation of the weakening effect magnitude at large currents. Molotskii obtains saturation by setting in (37) $j >> j_0$.

In the intermediate range of current densities, a linear dependence of stress drop on current density was observed. Molotskii shows that expression (37) in the vicinity of inflection point gives linear dependence:

$$\frac{\Delta\sigma(j)}{\sigma^*} = \frac{1}{4}\frac{j^2 R_0^2}{H_0^2}. \tag{43}$$

In order to find the change of stress applied to the whole conductor, the expression for the relative stress drop should be averaged over the cross-section of the conductor

$$\frac{\Delta\sigma(j)}{\sigma(0)} = \frac{1}{\pi R_0^2}\int \frac{\Delta\sigma(j,r)}{\sigma(0)} dS. \tag{44}$$

In case of small current density, substitution of (37a) gives

$$\frac{\Delta\sigma(j)}{\sigma(0)} = \int_0^{R_0} \frac{\left(r/R_0\right)^2}{\left(j_0/j\right)^2} d\frac{r^2}{R_0^2} = \frac{1}{2}\left(j/j_0\right)^2. \tag{45}$$

If we use expression (45) as the author does, then, we obtain

$$\frac{\Delta\sigma(j)}{\sigma(0)} = \int_0^{R_0} \frac{\left(r/R_0\right)^2}{\left(r/R_0\right)^2 + \left(j_0/j\right)^2} d\frac{r^2}{R_0^2} = 1 - \left(j_0/j\right)^2 \ln\left[1 + \left(j/j_0\right)^2\right]. \tag{46}$$

Now let $j << j_0$. Expanding the logarithm in a Tailor series, we get the same result as (45)

$$\frac{\Delta\sigma(j)}{\sigma(0)} \approx 1 - \left(j_0/j\right)^2 \left[ \left(j/j_0\right)^2 - \frac{1}{2}\left(j/j_0\right)^4 + \ldots \right] = \frac{1}{2}\left(j/j_0\right)^2 .$$

This result differs from (41) obtained by Molotskii by the factor of 1/2.

Conclusions regarding the linear dependence on current density and saturation cannot be obtained basing on (37), because it is necessary to go beyond the domain of applicability of the approximation with respect to which the formula has been obtained.

Let us now consider a general case, when magnetic field can be of any magnitude. Taking the expression for dislocation mean free path (32), we obtain

$$\frac{\Delta\sigma(H)}{\sigma(0)} = 1 - \sqrt{1 - \frac{2H^2}{H_0^2 + \alpha H^2}}. \tag{47}$$

Let us switch from magnetic field to current density using (40). Then, the expression for relative stress drop will have the following form

$$\frac{\Delta\sigma(j,r)}{\sigma(0)} = 1 - \sqrt{\frac{1 + (\alpha - 2)\left(j/j_0\right)^2 \left(r/R_0\right)^2}{1 + \alpha\left(j/j_0\right)^2 \left(r/R_0\right)^2}}. \tag{48}$$

In order to obtain stress drop, we average (48) over the sample cross-section

$$\frac{\Delta\sigma(j)}{\sigma(0)} = \frac{1}{\pi R_0^2}\int \frac{\Delta\sigma(j,r)}{\sigma(0)}\, dS = 1 - \int_0^{R_0} \sqrt{\frac{1 + (\alpha - 2)\left(j/j_0\right)^2 \left(r/R_0\right)^2}{1 + \alpha\left(j/j_0\right)^2 \left(r/R_0\right)^2}}\, d\left(\frac{r}{R_0}\right)^2 . \tag{49}$$

As a result, we get

$$\frac{\Delta\sigma(j)}{\sigma(0)} = 1 - \frac{1}{\alpha}\left(j/j_0\right)^2 \left[ \sqrt{\left(1 + (\alpha - 2)\left(j/j_0\right)^2\right)\left(1 + \alpha\left(j/j_0\right)^2\right)} - 1 + \right.$$

$$\left. + \frac{2}{\sqrt{\alpha(\alpha - 2)}} \ln \left| \frac{\sqrt{1 + (\alpha - 2)\left(j/j_0\right)^2} + \sqrt{(\alpha - 2)(1 + \alpha\left(j/j_0\right)^2)/\alpha}}{1 + \sqrt{(\alpha - 2)/\alpha}} \right| \right],$$

$$\frac{\Delta\sigma(j)}{\sigma(0)} = 1 - \left(j_0/j\right)^2 \left[S_1 + S_2\right] = 1 - \frac{1}{x}\left[S_1 + S_2\right], \quad x = \left(j/j_0\right)^2 . \tag{50}$$

Expressions for $S_1$ and $S_2$ and their expansions with respect to small $x$ are given below

$$S_1 = \frac{1}{\alpha}\left\{\sqrt{\left(1+(\alpha-2)x\right)\left(1+\alpha x\right)}-1\right\} \underset{x\to 0}{\approx} \frac{\alpha-1}{\alpha}x - \frac{1}{2\alpha}x^2,$$

$$S_2 = \frac{2}{\alpha^{\frac{3}{2}}\sqrt{\alpha-2}} \ln\left|\frac{\sqrt{1+\left(\alpha-2\right)\left(j/j_0\right)^2}+\sqrt{\frac{\alpha-2}{\alpha}\left(1+\alpha\left(j/j_0\right)^2\right)}}{1+\sqrt{\frac{\alpha-2}{\alpha}}}\right| \approx$$

$$\underset{x\to 0}{\approx} \frac{1}{\alpha}x - \frac{\alpha-1}{2\alpha}x^2 - \frac{1}{4}\sqrt{\frac{\alpha-2}{\alpha}}x^2.$$

In case of small current densities,

$$\frac{\Delta\sigma(j)}{\sigma(0)} \approx \frac{1}{2}\left(j/j_0\right)^2\left[1+\frac{1}{2}\sqrt{\frac{\alpha-2}{\alpha}}\right], \quad j << j_0. \tag{51}$$

For getting (45) or (46), we need to set $\alpha = 2$. However, all critical remarks do not disprove most part of author's conclusions. At small current density, the dependence of relative stress drop on current density is quadratic. Factor 1/2 in (45), (46), (51) that emerged as a result of averaging can, however, influence the author's statement about quantitative match with some experimental data.

In case of big current density, saturation indeed takes place:

$$\frac{\Delta\sigma(j)}{\sigma(0)} \to 1-\sqrt{\frac{\alpha-2}{\alpha}}, \quad j\to\infty.$$

Author states that predictions of his model qualitatively (and in some cases even quantitatively) match the experimental data. His model explains the following regularities of electroplastic effect: quadratic dependence of the effect magnitude on current density at small, linear dependence at intermediate and saturation at big current density. The dependence of the wire diameter is also explained.

### 4.3. Influence of Thermal Expansion on the Plasticization of Nonferromagnetic Materials

Deformation of metallic cylinders at conducting through them of high-density pulse electric current was considered [35]. Viscoplastic model that takes into account Joule heating and Lorentz force was built. This model is then applied for explanation of more early experimental results of other authors concerning electroplastic effect. In cases considered by authors, current pulses of 60–100 μs duration and ~ $10^5$ A/cm$^2$ density were conducted through wires of different metals during their

active strain at constant rate of ~ $10^{-4}$ $s^{-1}$. It was shown that, because of the size of the samples is small compared to skin depth, the current can be considered uniformly distributed over the sample cross-section. Pulse duration is small compared to characteristic thermal diffusion time and much greater than electric field diffusion time that allows regarding the heating as adiabatic.

It is stated that metal samples behaviour under the action of mechanical load and pulse current can be explained by means of well-known mechanisms of electric current influence, *i.e.* Joule heating and Lorentz force, where Lorenz force is secondary factor compared to Joule heating. Authors think involving of any additional concepts about interaction of electric current with dislocations to be redundant.

The proposed model presumes the following. At the conduction of current through the sample, it gets heating that is accompanied by thermal expansion. It means that between the pulse beginning and the moment of maximal heating, the sample changes its size at some rate. If the mentioned process takes place during plastic strain at constant rate, then, much less loading is needed to maintain this it, or it can be not required at all. Now, the strain rate of constant magnitude consists of two parts: plastic and elastic. According to Bilyk's estimations, plastic part of strain rate drops approximately on two orders. Therefore, spasmodic loading drop has to be observed. After pulse conduction, the sample will begin to cool down, and, consequently, mechanical stress will have to be increased. Now, elastic constituent of strain is negative. Plastic part, therefore, is increased. Bilyk *et al.* [35] presume the dependences of materials on plastic strain rate to play the key role. Because of heating occurs much faster than cooling down (during heating the heat is generated in all the volume of the sample, while the loss of heat is possible only through surface), the load increase during cooling of the sample is less by magnitude but more extended in time. According to the authors' estimations, thermal diffusion characteristic time for different metals samples with the given sizes is 2–4 orders greater than current pulse duration.

Unger *et al.* [36] prescribe the main part to expansion. They have performed their numerical calculations using two models: thermos-elasto-plastic and thermos-elasto-visco-plastic. The later one takes into account the dependence of plastic flow parameters on strain rate. Difference between the results of both models is small. Comparing to experimental data, the authors got a match with 5% error that can be partially explained because of the precise experimental pulse shape is unknown.

Authors suggest [36], that in order to get the complete answer to the question whether the electric current exerts some additional influence on plastic strain one needs to perform tests involving deformations of samples that are heated in nonelectrical ways during the deformation

process.

Remark: as the authors themselves [36] showed it, characteristic time of thermal diffusion (and correspondingly the time of heating through the surface) is of several orders greater than in case of heating by the current. Therefore, thermal expansion rate will also be smaller. Therefore, for obtaining precise analogy, we need not only the same heating magnitude but the corresponding heat rate as well.

Unger *et al.* [36] achieved the conclusion that direct influence of current on dislocations, if it exists, is of second order of smallness compared to the thermal expansion.

So, the effect that had been neglected before has been considered at completely different angle. Authors have payed attention not only to the magnitude of thermal expansion but also to the rate of the process, which makes sense because it is the value of strain rate that is constant in the experiments.

### 4.4. Nonequilibrium Electron–Phonon Kinetics Influence of Electroplasticity of Metals

All quantities are taken for nickel: $s = 2.96 \cdot 10^5$ cm/s is the transversal sound velocity, $n = 2.5 \cdot 10^{22}$ cm$^{-3}$ is the concentration of conductivity electrons, $\varepsilon_F = 5 \cdot 10^{-19}$ J, lattice constant $a = 3.5 \cdot 10^{-8}$ cm, $\rho_s$ is specific residual resistance, measured in experiment $\rho_s^{-1} = 2.27 \cdot 10^6$ S/cm, $T_e = T_0 = 77$ K. Creep rate, observed in tests before turning on of magnetic field was equal to $2.8 \cdot 10^{-6}$ s$^{-1}$, $3.67 \cdot 10^{-6}$ s$^{-1}$, $5.5 \cdot 10^{-6}$ s$^{-1}$ for the stress values of 230 MPa, 270 MPa and 330 MPa correspondingly. These values can be obtained from the equations (1) and (2) using the following quantities: $b = 3.52 \cdot 10^{-8}$ cm, $l = 2.25 \cdot 10^{-6}$ cm, $\rho_d = 1 \cdot 10^9$ cm$^{-2}$, $\nu_d^0 = 1.8 \cdot 10^{12}$ s$^{-1}$, $T = 77$ K, potential pit depth $U = 0.22$ eV, $H(\sigma^*) = U - \sigma V$, activation volume $V = 7.26 \cdot 10^{-24}$ cm$^3$. For explanation of the creep rate jump observed after turning on of magnetic field by heating, temperature growth should have been of approximately 18 K. For our characteristic electric field, we have the eddy current density of $j = 3.5 \cdot 10^5$ A/cm$^2$. According to [3, 4], at such current density, EPE takes place during tens of μs. In those experiments, strain rate was constant and equal to $10^{-4}$ s$^{-1}$ and the stress drop caused by the conduction of current pulses was of several %. In our tests, as it can be seen from Figs. 1–3, at constant stress, the strain rate jump had the magnitude of $10^{-3}$ s$^{-1}$. Effect of periodic monopolar pulses is much greater than in case of single pulse with much longer growth time (see Figs. 1–3).

## 5. CONCLUSION

1. The necessity of kinetic consideration of nonequilibrium dynamics

of electron-phonon subsystem of a crystal in a strong electric field was justified.
2. A method of numerical solution of Boltzmann kinetic equations' set for electron and phonon distribution function without expanding electron distribution function with respect to phonon energy has been proposed.
3. It has been shown that, under the influence of strong electric field, electron distribution function gets nonequilibrium in the vicinity of Fermi energy, and due to electron–phonon collisions, substantial energy transfers to phonon subsystem forming nonequilibrium phonon distribution function. Based on the Granato–Lücke and Landau–Hoffmann modified models and using the calculated phonon distribution function, it was shown that the force exerted by phonons upon dislocations is greater than in case of thermodynamically equilibrium heating of the sample by 12 K observed in experiment.
4. Comparison between results of calculation and experimental data for nickel at the observed values of experimental parameters has clearly demonstrated that the proposed approach gives results of the same order of magnitude that the experiment.
5. So, weakening of nickel under the influence of stationary or nonstationary magnetic field manifests itself at plastic flow that is known to be caused by the presence and motion of mobile dislocations in crystal. Therefore, the mechanism of magnetic field influence on plastic properties of the material are obviously connected with its influence on dynamic characteristics of dislocations.
6. We have deliberately conducted experimental research on nonstationary (constant sign and varying magnitude) magnetic field influence under the conditions of stationary temperature in order to exclude the contribution to dislocations mobility change an adding of magnetic field from the interaction of dislocations with the mobile domain boundaries and from thermal effects. At remagnetization, the mobile boundaries are known to interact with dislocations by helping them to overcome local obstacles, causing the increase of mobile dislocations density and creep strain.

As it is shown, remarkable contribution to the effects of weakening under the influence of magnetic field can be made by Joule heating by eddy currents at magnetic field alterations.

Therefore, four different approaches to explanation of electroplastic effect have been reviewed. Each one is based on different mechanisms of electric current influence on strain. The theories not only cannot be expressed one through other, but they also do not exclude one another. So, for example, thermal expansion at big rate, that is told of by Bilyk *et al.* and Unger *et al.* [34, 35], does not prohibit the magnetic field influence upon the spins of dopants and pinned dislocation cores, that are involved in Molotskii's model [32–34]. Other

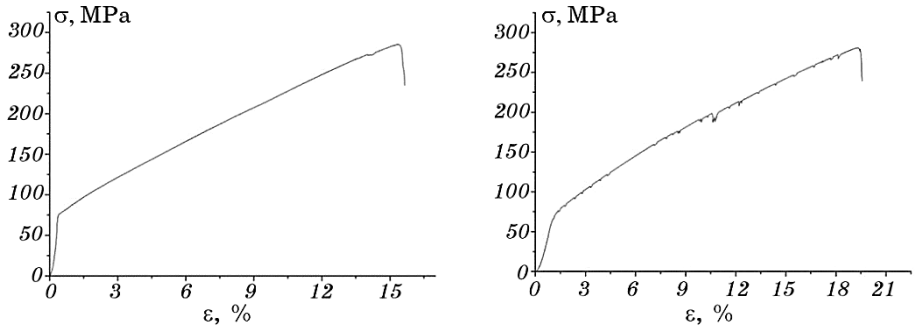


**Fig. 6.** Dependence of the polycrystalline nickel flow stress on the relative strain: left plot—without of additional action of the electric current; right plot—with periodic action of pulse electric current with density of $2.75 \cdot 10^5$ A/cm$^2$.

mechanisms are also not discarded. For example, none of the above-mentioned theories contradicts to enhanced phonon generation of short-wave phonons by nonequilibrium electrons that, in turn, effectively depinning dislocations from stoppers. Therefrom follows the necessity of performing more experimental investigations in order to prove/disprove each of the theories separately. At planning of experiments, the following important questions are to be solved.

For checking Bilyk's *et al.* model [35, 36], it is necessary to separate fast heating from electromagnetic influence.

For checking Molotskii's *et al.* model [32–34], it is necessary to carry out tests on the materials without paramagnetic dopants.

7. For estimation of the contribution from the induction part of electric field, which is caused by monopolar magnetic field change, an experimental study of the influence of pulse current density of flow stress decrease during current pulses has been carried out. Comparative experiments were conducted on the similar samples of high purity (99.996%) polycrystalline nickel. Parameters of electric current density corresponded to the induction electric field strength generated by monopolar pulses of magnetic field at creep tests (see Sect. 2). As it is seen from Fig. 6 (right plot), during the current pulse, $\cong 1\%$ decrease of flow stress takes place that corresponds to 0.1% strain. These data correspond to experimental results presented on Figs. 1–4.

## ACKNOWLEDGEMENTS

This work is financially supported in part by the National Academy of Sciences of Ukraine (under the contract 61-02-14) within the frame collaboration between the National Academy of Sciences of Ukraine and Russian Foundation for Basic Research (under the contract 14-02-90248).

## REFERENCES


1. S. Hayashi, S. Takahashi, and M. Yamamoto, *J. Phys. Soc. Jpn.*, **25**, No. 2: 910 (1968); *J. Phys. Soc. Jpn.*, **30**: 381 (1971).
2. I. A. Gindin, I. S. Lavrinenko, and I. M. Neklyudov, *JETP Lett.*, **16**, No. 6: 341(1972); *Fizika Tverdogo Tela*, **15**, No. 4: 636 (1973) (in Russian).
3. O. A. Troitskii and V. I. Likhtman, *Dokl. Akad. Nauk SSSR*, **148**, No. 2: 332 (1963) (in Russian).
4. V. E. Gromov, V. Ya. Tsellermayer, and V. I. Bazaykin, *Elektrostimulirovannoye Volocheniye: Analiz Protsessa i Mikrostruktura* (Moscow: Nedra: 1996) (in Russian).
5. V. I. Spitsyn and O. A. Troitskii, *Elektroplasticheskaya Deformatsiya Metallov* (Moscow: Nauka: 1985) (in Russian).
6. V. V. Stolyarov, *Vestnik Nauchno-Tekhnicheskogo Razvitiya*, No. 67: 35 (2013) (in Russian).
7. R. B. Morgunov, *Physics–Uspekhi*, **47**, No. 2: 131 (2004).
8. I. M. Nekludov, V. M. Azhazha, K. A. Yushchenko, V. I. Sokolenko, A. V. Mats, V. M. Netesov, and V. V. Vartanov, *Fizika i Khimiya Obrabotki Materialov*, No. 1: 84 (2011) (in Russian).
9. V. P. Lebedev and S. V. Savych, *Vestnik KhNU. Seriya 'Fizika'*, No. 962, Iss. 15: 88 (2011) (in Russian).
10. I. A. Gindin, S. F. Kravchenko, and Ya. D. Starodubov, *Pribory i Tekhnika Eksperimenta*, No. 3: 269 (1963) (in Russian).
11. V. K. Aksenov, I. A. Gindin, V. P. Lebedev, and Ya. D. Starodubov, *Fizika Nizkikh Temperatur*, **6**, No. 1: 118 (1980) (in Russian).
12. V. K. Aksenov, I. A. Gindin, E. I. Druinskii, E. V. Karaseva, and Ya. D. Starodubov, *Fizika Nizkikh Temperatur*, **3**, No. 7: 922 (1977) (in Russian).
13. I. M. Nekludov, Ya. D. Starodubov, and V. I. Sokolenko, *Ukrayinskyy Fizychnyy Zhurnal*, **50**, No. 8A: A113 (2005) (in Russian).
14. C. R. Chow and E. Nembach, *Acta Met.*, **24**, No. 5: 453 (1976).
15. V. K. Aksenov, I. A. Gindin, E. V. Karaseva, and Ya. D. Starodubov, *Fizika Nizkikh Temperatur*, **4**, No. 10: 1316 (1978) (in Russian).
16. D. N. Bolshutkin, V. A. Desnenko, and V. Ya. Illichev, *Fizika Nizkikh Temperatur*, **2**, No. 2: 256 (1976) (in Russian).
17. D. N. Bolshutkin, V. A. Desnenko, and V. Ya. Illichev, *Fizika Nizkikh Temperatur*, **2**, No. 12: 1544 (1976) (in Russian).
18. M. A. Vasiliev, *Usp. Fiz. Met.*, **8**, No. 1: 65 (2007) (in Russian).
19. M. I. Kaganov, V. Ya. Kravchenko, and V. D. Natsik, *Physics–Uspekhi*, **16**, No. 6: 878 (1974).
20. I. M. Neklyudov and N.V. Kamyshanchenko, *Fizicheskie Osnovy Prochnosti i Plastichnosti Metallov. Part 2: Defekty v Kristallakh* (Moscow–Belgorod: Izd-vo Belgorodskogo GU: 1997) (in Russian).
21. A. I. Landau and Yu. I. Gofman, *Fizika Tverdogo Tela*, **16**, No. 11: 3427 (1974) (in Russian).
22. A. Granato and K. Lücke, *J. Appl. Phys.*, **27**, No. 5: 583 (1956).
23. V. I. Dubinko, V. I. Karas, V. F. Klepikov, P. N. Ostapchuk, and I. F. Potapenko, *Voprosy Atomnoy Nauki i Tekhniki. Seriya 'Fizika Radiatsionnykh Povrezhdenij i Radiatsionnoye Materialovedenie'*, **4–2** (94):

158 (2009) (in Russian).
24. V. E. Zakharov and V. I. Karas', *Physics–Uspekhi*, **56**, No. 1: 49 (2013).
25. V. I. Karas', A. M. Vlasenko,V. N. Voyevodin, V. I. Sokolenko, and V. E. Zakharov, *East Europe Physical Journal*, **1**, No. 1: 40 (2014).
26. N. Perrin and H. Budd, *Phys. Rev. Lett.*, **28**, No. 26: 1701 (1972).
27. V. I. Karas', A. M. Vlasenko, V. I. Sokolenko, and V. E. Zakharov, *JETP*, **121**, No. 3: 499 (2015).
28. V. I. Karas', A. M. Vlasenko, A. G. Zagorodniy, and V. I. Sokolenko, *Proc. Int. Conf. MSS-14 'Mode Conversion, Coherent Structure and Turbulence' (Nov. 24–27, 2014)* (Moscow: LENAND: 2014), p. 64.
29. V. E. Zakharov, V. I. Karas', and A. M. Vlasenko, *Proc. Int. Conf. MSS-14 'Mode Conversion, Coherent Structure and Turbulence' (Nov. 24–27, 2014)* (Moscow: LENAND: 2014), p. 34.
30. V. I. Karas', V. I. Sokolenko, E. V. Karasyova, A. V. Mats, and A. M. Vlasenko, *Problems of Atomic Science and Technology. Series: Plasma Electronics and New Acceleration Methods*, No. 4 (98): 277 (2015).
31. A. F. Sprecher, S. L. Mannan, and H. Conrad, *Acta Mater.*, **31**, No. 7: 1145 (1986).
32. M. Molotskii and V. Fleurov, *Phys. Rev. B*, **52**, No. 22: 829 (1995).
33. M. Molotskii and V. Fleurov, *Phys. Rev. Lett.*, **78**, No. 14: 2779 (1997).
34. M. I. Molotskii, *Mater. Sci. Eng. A*, **287**: 248 (2000).
35. S. R. Bilyk, K. T. Ramesh, and T. W. Wright, *J. Mechanics Phys. Solids*, **53**: 525 (2005).
36. J. Unger, M. Stiemer, L. Walden, F. Bach, H. Blum, and B. Svendsen, *Proc. 2nd Int. Conf. on High Speed Forming (20–21 March, 2006, Dortmund)* (Germany, Dortmund: Institut für Umformtechnik und Leichtbau: 2006), p. 23.